

Pharmacodynamic study of axitinib in patients with advanced malignancies assessed with ^{18}F -3'-deoxy-3'-fluoro-L-thymidine positron emission tomography/computed tomography

Justine Yang Bruce¹ · Peter Colin Scully² · Lakeesha L. Carmichael³ ·
Jens C. Eickhoff³ · Scott B. Perlman⁴ · Jill Marie Kolesar⁵ · Jennifer L. Heideman⁶ ·
Robert Jeraj⁷ · Glenn Liu¹

Received: 28 January 2015 / Accepted: 8 May 2015 / Published online: 29 May 2015
© Springer-Verlag Berlin Heidelberg 2015

Abstract

Purpose Rapid disease progression associated with increased tumor proliferation has been observed during withdrawal of anti-angiogenic therapy. We characterize the dynamics of withdrawal flare for axitinib.

Methods Thirty patients with metastatic solid malignancies received axitinib for 2 weeks, followed by a 1-week drug holiday. Twenty patients suitable for PET imaging received scans with ^{18}F -3'-deoxy-3'-fluoro-L-thymidine (FLT), a marker of proliferation. Plasma VEGF and axitinib

pharmacokinetic levels were also assessed at specified time points.

Results During axitinib withdrawal, significant increases in both SUV_{max} (+22 %; $p = 0.006$) and SUV_{mean} (+20 %; $p = 0.001$) were observed. Significant increases relative to peak axitinib concentration were observed at day 2 withdrawal for SUV_{max} and SUV_{mean} , with no further significant increase from day 2 to day 7 of withdrawal. No significant change in SUV_{max} or SUV_{mean} was observed during the treatment period, relative to baseline. VEGF concentration significantly increased when on drug ($p < 0.001$) and decreased back to a level indistinguishable from baseline

Justine Yang Bruce and Peter Colin Scully have contributed equally to the research and writing of the manuscript.

✉ Justine Yang Bruce
jybruce@medicine.wisc.edu

Peter Colin Scully
pscully@wisc.edu

Lakeesha L. Carmichael
lcarmichael@biostat.wisc.edu

Jens C. Eickhoff
eickhoff@biostat.wisc.edu

Scott B. Perlman
sb.perlman@hosp.wisc.edu

Jill Marie Kolesar
jmcolesar@pharmacy.wisc.edu

Jennifer L. Heideman
jlv@medicine.wisc.edu

Robert Jeraj
rjeraj@wisc.edu

Glenn Liu
gxl@medicine.wisc.edu

² Department of Medical Physics, University of Wisconsin, 1111 Highland Ave, Madison, WI 53705, USA

³ Department of Biostatistics and Medical Informatics, University of Wisconsin, MC 4675, K6/422 Clinical Science Center, 600 Highland Ave, Madison, WI 53792, USA

⁴ Department of Radiology, University of Wisconsin, Clinical Science Center, 600 Highland Ave, Box 3252, Madison, WI 53792, USA

⁵ Department of Pharmacy, University of Wisconsin, K4/554 Clinical Science Center, 600 Highland Ave, Madison, WI 53792, USA

⁶ University of Wisconsin Carbone Cancer Center, Clinical Science Center, 600 Highland Ave, Box 5666, Madison, WI 53792, USA

⁷ Department of Medical Physics, University of Wisconsin, Rm7033 Wisconsin Institute Medical Research, 1111 Highland Ave, Madison, WI 53705, USA

¹ Department of Medicine, University of Wisconsin Carbone Cancer Center, 7105 Wisconsin Institute Medical Research, 1111 Highland Ave, Madison, WI 53705, USA

by day 7 of drug washout ($p = 0.448$). No correlation between change in VEGF and change in imaging metrics was observed.

Conclusions A significant increase in tumor proliferation was observed during withdrawal of axitinib therapy, and this flare occurred within 2 days of axitinib withdrawal. An exploratory analysis indicated that this flare may be associated with poor clinical outcome.

Keywords Axitinib · Pharmacodynamic · FLT PET/CT · Angiogenesis inhibitors · Tyrosine kinase inhibitors

Introduction

Despite significant improvements in the treatment of solid malignancies, most patients unfortunately experience disease progression and ultimately die of their disease. It is therefore of the utmost importance to develop new therapeutic approaches, whether through discovery of new treatment regimens or through improved matching of patients with treatments that currently exist through personalized medicine. Molecular imaging is an important tool in this endeavor, to characterize both treatment effects and treatment efficacy.

Angiogenesis, the process by which tumors develop vascular structure, is known to be required for tumor growth and progression, making it an attractive target for cancer therapy [6, 7]. The best-described target of anti-angiogenic therapy is the vascular endothelial growth factor (VEGF) signaling pathway [7]. In the decades since VEGF's initial discovery [20], many targeted therapies against this pathway have been developed and approved. Bevacizumab was initially developed as a monoclonal antibody against VEGF, but it showed low single-agent activity in solid malignancies [3, 8]. Tyrosine kinase inhibitors (TKIs) that target the VEGF receptors (VEGFRs) were subsequently developed, and these showed greater single-agent activity. Several VEGFR TKIs (sorafenib, pazopanib, and sunitinib) have been approved for the treatment of certain solid malignancies, including metastatic renal cell carcinoma [5, 14, 22], hepatocellular carcinoma [13], and gastrointestinal stromal tumors [24]. Axitinib is a potent second-generation VEGFR TKI that inhibits VEGFR 1, 2, and 3 without inhibiting other targets, such as platelet-derived growth factor receptors, KIT, and FLT-3 [15, 17]. The relative potency of axitinib is 50–450 times greater than that of other first-generation VEGFR TKIs, making it a promising anti-angiogenic agent with fewer off-target toxicities [21]. Axitinib is now approved for the treatment of metastatic renal cell carcinoma in patients who failed prior systemic chemotherapy [16]. Several trials have combined axitinib with conventional chemotherapy, but the combinations studied

thus far have not been proven to be effective: axitinib plus gemcitabine was not found to improve overall survival for patients with advanced pancreatic adenocarcinoma [9], and in patients with breast cancer, the addition of axitinib to docetaxel was not found to increase time to progression [19]. These negative findings may indicate that VEGFR TKI therapy induces a tumor response that is antagonistic to conventional chemotherapy, when the two are given in combination.

A potential source of this antagonistic effect could be “withdrawal flare,” a period of rapid tumor growth and disease progression following cessation of treatment with VEGFR TKI therapy [12, 18]. This has been described clinically for patients with a wide variety of advanced solid malignancies, including in the kidneys [12], lung [11], and thyroid [26]. Although the detailed biological mechanisms of withdrawal flare are unknown, increased cellular proliferation is certainly a key component of rapid tumor regrowth. Positron emission tomography (PET) imaging with the proliferation marker ^{18}F -3'-deoxy-3'-fluorothymidine (FLT)—whose uptake measures thymidine kinase 1 activity [20], and whose correlation with the gold standard Ki-67 immunohistochemical proliferation marker is both significant and independent of cancer type [2]—provides an excellent means of assessing tumor response to TKI treatment and cessation. This is especially true over the relatively short time scales of withdrawal flare, where functional imaging tends to be more responsive than anatomical imaging [25].

A recent study used FLT PET to assess the proliferative response of solid tumors to cessation of sunitinib therapy [12]. In many patients, a decrease in tumor FLT uptake during sunitinib treatment was followed by a significant increase in uptake during scheduled treatment breaks. This response pattern suggests that tumors exhibit decreased proliferation during VEGFR TKI therapy, which may be antagonizing cell cycle-specific chemotherapy given in combination, while at the same time priming tumors for rapid progression following TKI cessation [12].

The primary objective of the present study was to observe and quantify pharmacodynamic changes associated with axitinib withdrawal in patients with solid malignancies, using FLT PET imaging. In particular, we assess the change in FLT uptake following cessation of axitinib treatment, to determine whether axitinib withdrawal is associated with a proliferative flare response. We further characterize the temporal dynamics of this phenomenon, in order to understand how axitinib might be deployed more effectively in combination therapy. Finally, this study also investigates the relationship between quantitative biomarkers of axitinib withdrawal flare and treatment outcome, in order to explore their potential as indicators of patient prognosis or disease resistance.

Patients and methods

Patient selection

Patients were required to have histologically or cytologically confirmed advanced solid malignancies (excluding lymphoma) that were metastatic or unresectable and for which no standard curative therapy existed. All patients were required to have measurable disease by RECIST 1.0 criteria and also at least one metastatic lesion that was appropriate for FLT PET/CT imaging [23]. Other key inclusion criteria included normal organ and marrow function, and well-controlled blood pressure (<140/90 mm Hg). Exclusion criteria included therapeutic doses of coumarin-derivative anticoagulants (although low molecular weight heparin was allowed provided that the INR was ≤ 1.5), pre-existing thyroid abnormality, known brain metastases, and patients taking potent inducers or inhibitors of CYP3A4 liver enzyme. Steroid use was not recommended during axitinib treatment. All patients signed informed consent documents approved by the Institutional Review Board at the University of Wisconsin. This study was conducted in accordance with the Declaration of Helsinki.

Drug administration and study design

The full trial schematic is shown in Fig. 1. While on therapy, patients were treated with axitinib at a dose of 5 mg orally, twice daily, taken with food. Each cycle of axitinib treatment was 21 days in duration. For cycle 1 only, patients were instructed to take axitinib for 14 days, followed by a drug holiday of 1 week (at least 7 days). For all subsequent cycles, patients received axitinib continuously, without any scheduled drug breaks. Axitinib was provided by the sponsor.

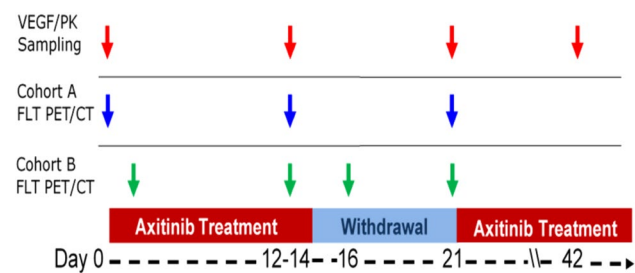


Fig. 1 Trial schematic. Red arrows indicate plasma sampling, which are analyzed for circulating VEGF and axitinib PK levels; Blue arrows indicate FLT PET/CT imaging for patients in cohort A; Green arrows indicate FLT PET/CT imaging for patients in cohort B. All patients receive imaging at peak axitinib exposure (day 12 to day 14), and at the end of withdrawal (day 21)

Plasma VEGF/PK sampling

Plasma samples were drawn prior to axitinib therapy, at peak drug concentration (day 12 to day 14), at the end of the drug washout (day 21), and at the beginning of cycle 3 (week 6; see Fig. 1). Samples were evaluated for concentration of VEGF, using a commercially available 96-well plate quantitative sandwich immunoassay (Quantikine human VEGF, R&D Systems); samples were also analyzed for circulating axitinib levels and to evaluate drug pharmacokinetics (PK), as previously described [12].

FLT PET/CT imaging

Each patient received a series of three FLT PET/CT scans during the first cycle of axitinib therapy (Fig. 1). All patients received FLT PET/CT scans at peak concentration of axitinib (day 12 to day 14) and at the end of the drug holiday (day 21), to assess the primary endpoint of FLT response during the withdrawal period. For the third scan, patients were divided into two cohorts, with patients in cohort A receiving an FLT PET/CT scan at baseline (day -3 to day 0) and patients in cohort B receiving an FLT PET/CT scan on the second day of drug washout (day 16).

Patients were scanned on a Discovery VCT (General Electric) PET/CT scanner. At each imaging time point, patients first received a low-dose noncontrast CT scan, which was used for attenuation correction. Patients then received a static whole-body PET scan (seven bed positions, 5 min per bed position, ~100 cm total axial field of view) beginning 60 min post-injection. Scans were acquired in three-dimensional mode and reconstructed using the ordered subsets expectation maximization iterative reconstruction algorithm with a 256×256 matrix size, 35 subsets, 2 iterations, and a 3-mm Gaussian post-filter.

The whole-body FLT PET/CT image was used to identify metastatic lesions for analysis. For each patient, up to four lesions were identified on the FLT PET/CT scan by an experienced nuclear medicine physician, and tumor regions of interest (ROIs) were manually segmented. These tasks were performed by the same individual for all patients on the study, to eliminate inter-observer variability. PET images were converted to standardized uptake values (SUV) following normalization to injected activity and patient weight. Within each lesion ROI, various SUV measures of FLT uptake were analyzed (SUV_{mean} , SUV_{max} , SUV_{peak} , and SUV_{total}), in order to fully characterize lesion response. For patients with multiple lesions, the average response of all evaluable lesions was calculated.

Table 1 Patient demographics

Characteristic	<i>n</i> = 30
Age (years)	
Median (range)	65 (44–78)
Number of patients	
Gender	
Female	7
Male	23
Primary disease site	
Prostate	6
Kidney	4
Colon	4
Lung	4
Head/neck	3
Pancreas	2
Other	7
Number of organs with metastases	
1	13
2	13
3+	4

Treatment response evaluation

Patients were evaluated for response and progression after every three cycles (every 9 weeks) of therapy using RECIST 1.0 guidelines [23]. An exploratory analysis was added to categorize patients by clinical benefit (CB) status (yes/no). We defined clinical benefit as those patients who remained on axitinib beyond 6 months. Patients who discontinued axitinib at month 6 or sooner for any reason (including progression, toxicity, and patient/physician discretion) were categorized as having no clinical benefit (NCB). The rationale for defining clinical benefit this way is due to the wide variety of solid tumor histologies represented in the recruitment population. Because of the large range in progression-free survival among different solid tumors, we chose a progression-free survival of 6 months as unequivocally beneficial. The FLT PET/CT imaging data were analyzed for correlation with patients' CB status.

Statistical methods

FLT SUV imaging metrics and plasma VEGF and axitinib PK levels were summarized in terms of medians and ranges at each measurement time point. Changes between baseline, peak axitinib exposure, and axitinib withdrawal measurement time points were evaluated using a nonparametric Wilcoxon signed-rank test. Associations between changes in imaging metrics and changes in plasma VEGF and axitinib PK levels were analyzed using Spearman's rank correlation analysis. In an exploratory analysis, the comparison

of changes in imaging metrics between those with clinical benefit (>6-month PFS) and those without clinical benefit (\leq 6-month PFS) was evaluated using a nonparametric Wilcoxon rank-sum test. All analyses were performed using SAS software version 9.3 (SAS Institute, Cary, NC). P values less than 0.05 were considered statistically significant.

Results

Patient characteristics

From July 2009 to October 2012, 30 patients were enrolled at the University of Wisconsin Carbone Cancer Center (Table 1). Of 30 enrolled patients, 20 were able to be fully characterized via PET imaging, and 24 patients had some, but not all data for pharmacodynamic analysis. An evaluable patient was defined as a subject who received all three FLT PET/CT scans per protocol and at least 90 % of axitinib doses prior to completion of FLT PET/CT scan #3. Reasons for patients being non-evaluable were as follows: incomplete sets of PET/CT scans due to technical difficulties, patients unwilling to undergo the last PET/CT scan secondary to treatment intolerance, and metastatic lesions that were not FLT avid. Thirteen evaluable patients were imaged on cohort A, and eleven evaluable patients were imaged on cohort B.

Disease response and efficacy

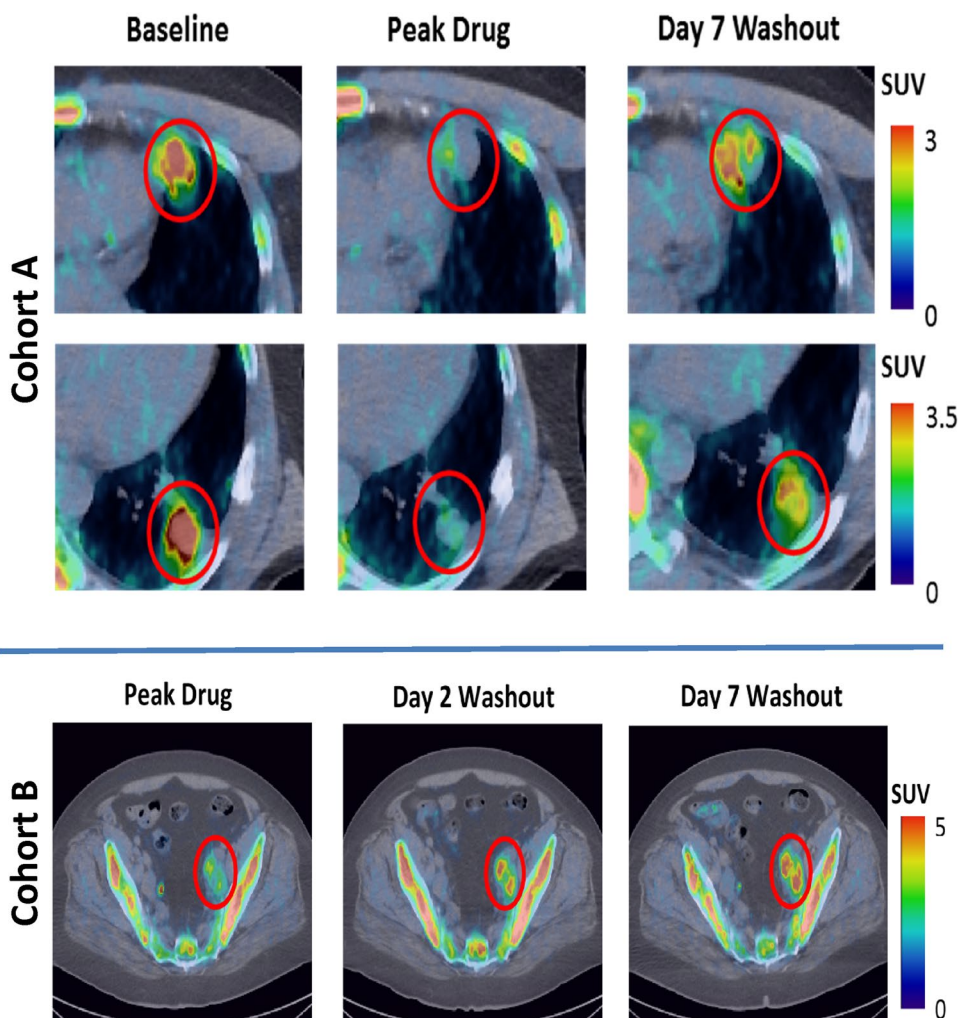
All thirty patients were evaluated for treatment effect and response by RECIST version 1.0 [23]. At best response, six patients had partial response, nineteen patients had stable disease, and five patients developed disease progression. For the exploratory clinical benefit analysis, only those patients who were evaluable for pharmacodynamic analysis were evaluated. Five patients were classified as having clinical benefit (6-month PFS) (cohort A = 1, cohort B = 4). Nineteen patients were classified as having no clinical benefit (cohort A = 12, cohort B = 7).

FLT PET/CT imaging

We have included representative images of the withdrawal flare phenomenon as imaged by FLT PET/CT for both imaging cohorts (Fig. 2). Quantitative imaging results are shown in Fig. 3, for both individual patients and the population medians. Although many additional quantitative imaging metrics were analyzed, we present only SUV_{max} and SUV_{mean} , as these likely capture different aspects of tumor proliferation and response.

The quantitative results are plotted in Fig. 3 and summarized in Table 2. Highly significant increases in both

Fig. 2 FLT PET/CT images of representative patients. *Top* cohort A patient, with head and neck carcinoma and multiple pulmonary and pleural metastases (two lesions shown). Decrease in FLT uptake is observed during axitinib treatment, followed by substantial increase during the withdrawal period. *Bottom* cohort B patient, with a carcinoma of unknown origin and extensive lymphadenopathy in the pelvic area. Increase in FLT uptake relative to peak drug is visible on the second day of washout and persists through the seventh day of washout. Both patients progressed six or fewer months after the start of axitinib therapy and are classified as having no clinical benefit. FLT uptake in normal bone marrow is also observed



SUV_{max} ($p = 0.006$) and SUV_{mean} ($p = 0.001$) are seen during the withdrawal period across all patients. The temporal dynamics of this effect are such that by day 2 of withdrawal, significant increases in both SUV_{max} ($p = 0.032$) and SUV_{mean} ($p = 0.019$) are observed, but no further significant increase is seen to occur later in the washout period (SUV_{max} $p = 0.193$; SUV_{mean} $p = 0.232$). No significant change in either SUV_{max} or SUV_{mean} was observed during axitinib treatment, relative to uptake levels at baseline.

Plasma VEGF and axitinib pharmacokinetics

Blood samples were collected at baseline, at peak axitinib concentration, at the end of the axitinib withdrawal period, and at the beginning of cycle 3 of axitinib therapy (see Fig. 1). Samples were analyzed for level of plasma VEGF, and the results are summarized in Fig. 4. The plasma VEGF levels increased significantly from baseline to the time of peak exposure ($p < 0.001$) and dropped significantly by the end of the withdrawal period ($p < 0.001$). At the beginning of cycle 3, plasma VEGF levels had significantly increased

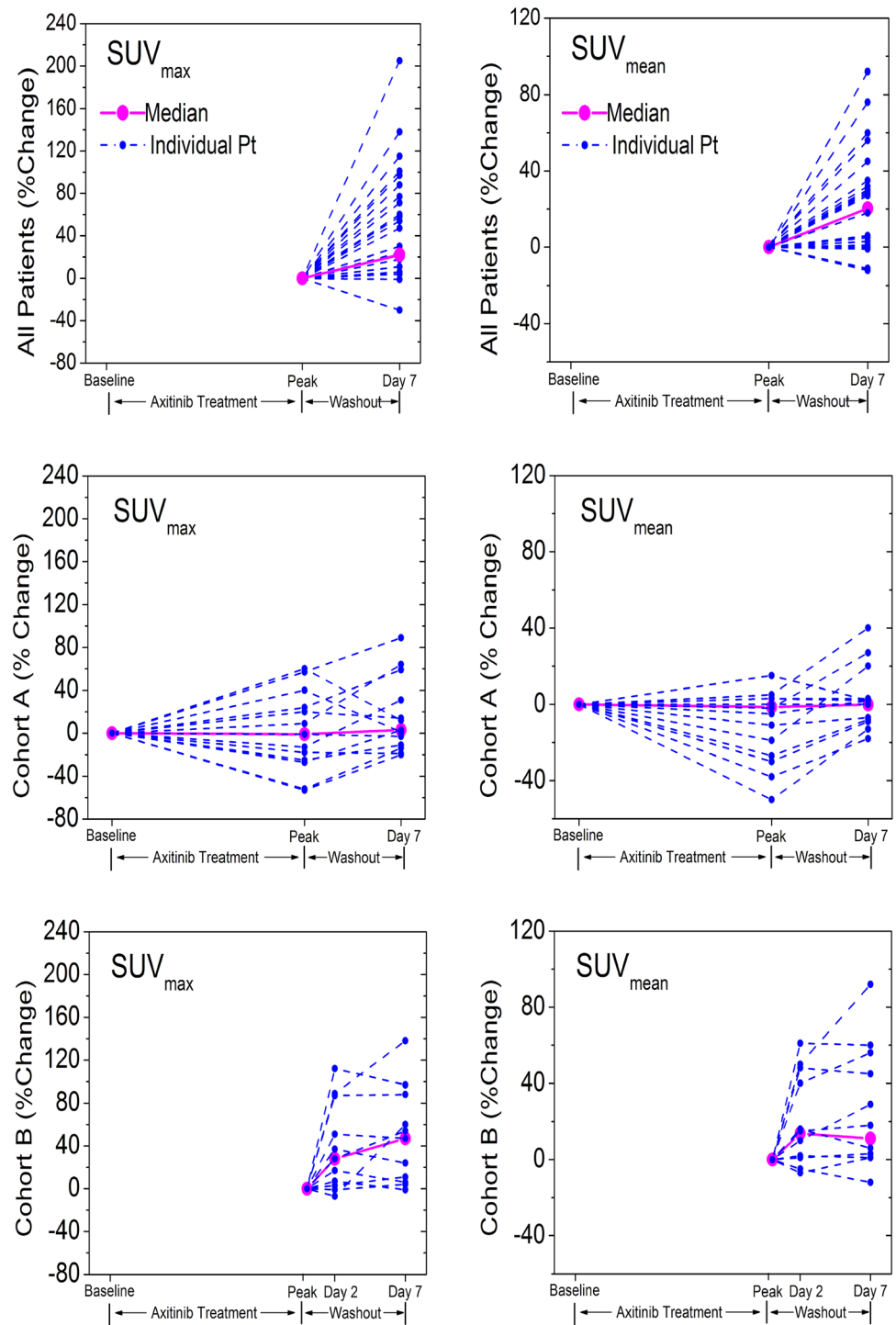
once again relative to baseline (+105 %, range -39 to $+732$; $p < 0.001$). The VEGF levels at the start of cycle 3 are not significantly different ($p = 0.42$) from the VEGF levels found at the peak drug time point of cycle 1.

Changes in axitinib PK were also evaluated and summarized in Table 2. There was a significant increase in the plasma axitinib concentrations from baseline to peak axitinib exposure (median 14 ng/mL; $p < 0.001$), followed by a significant decrease from peak axitinib exposure to the withdrawal (median -15 ng/mL; $p < 0.001$).

Correlation between plasma VEGF, pharmacodynamic imaging, and response parameters

The correlations for the change from peak axitinib exposure to withdrawal between the VEGF/PK and pharmacodynamic imaging were assessed using Spearman's rank correlations. There was no significant correlation between VEGF and SUV_{mean} , but a negative correlation between VEGF and SUV_{max} ($r = 0.045$; $p = 0.051$). There was no significant correlation between axitinib concentration and SUV_{mean} or SUV_{max} .

Fig. 3 Relative change in SUV_{mean} and SUV_{max} during the first cycle of axitinib therapy (2-week treatment, 1-week washout). *Top row* both cohorts (normalized to peak axitinib exposure). *Middle row* cohort A (normalized to pre-treatment). *Bottom row* cohort B (normalized to peak axitinib exposure). *Dotted lines* show individual patients. *Solid lines* show median response



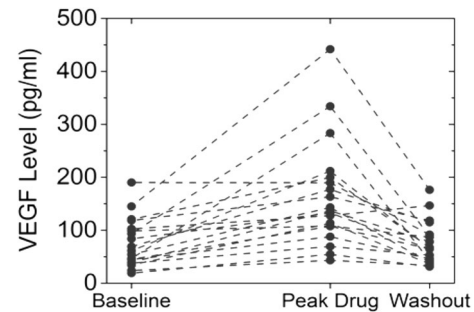
An exploratory analysis was performed to assess the association between changes in pharmacodynamic imaging with our classification of clinical benefit. In patients classified as having no clinical benefit (<6-month PFS), we observed a significant flare at day 7 of withdrawal relative to peak axitinib concentration ($SUV_{max} +28\%$; $p = 0.011$;

$SUV_{mean} +26\%$; $p = 0.003$). In patients who were classified as deriving clinical benefit, we found no significant increase in FLT uptake during the withdrawal period ($SUV_{max} +8\%$; $p = 0.25$; $SUV_{mean} +4\%$; $p = 0.63$). However, a Wilcoxon rank-sum test showed no significant difference between the two groups ($SUV_{max} p = 0.6$; $SUV_{mean} p = 0.3$).

Table 2 Summary of change in quantitative biomarkers over the course of axitinib therapy

	Time points	<i>n</i>	Median	Range	<i>p</i> value
Percentage change in imaging parameters, all patients					
Biomarker					
SUV _{max}	Washout (D7/peak)	20	22.1	−30–136	0.006
SUV _{mean}	Washout (D7/peak)	20	20.3	−12–90	0.001
Change in VEGF/PK, all patients					
VEGF/PK					
Axitinib C _{ss} (ng/mL)	Treatment (peak/base)	23	14	0–57	<0.001
	Washout (D7/peak)	20	−15	−57–0	<0.001
VEGF (%)	Treatment (peak/base)	22	117	−21–508	<0.001
	Washout (D7/peak)	20	−49	−85–15	<0.001
Percentage change in imaging parameters, cohort A					
Biomarker					
SUV _{max}	Treatment (peak/base)	10	−11.5	−71–60	0.492
	Full cycle (D7/base)	11	−0.7	−31–37	0.831
	Washout (D7/peak)	10	27.4	−30–136	0.084
SUV _{mean}	Treatment (peak/base)	10	−1.4	−63–17	0.375
	Full cycle (D7/base)	11	−0.1	−38–39	0.966
	Washout (D7/peak)	10	26.1	−11–76	0.049
Percentage change in imaging parameters, cohort B					
Biomarker					
SUV _{max}	Early washout (D2/Peak)	11	17.3	−15–87	0.032
	Total washout (D7/peak)	10	17.1	−8–119	0.049
	Late washout (D7/D2)	10	6.4	−13–72	0.193
SUV _{mean}	Early washout (D2/peak)	11	13.7	−7–61	0.019
	Total washout (D7/peak)	10	11.1	−12–90	0.020
	Late washout (D7/D2)	10	2.4	−9–27	0.232

The Wilcoxon signed-rank test is used for comparing the change between time points during each period. Percent change is used for SUV_{max}, SUV_{mean}, and VEGF; absolute change is used for axitinib PK. C_{ss} = concentration at steady state; Base = baseline (day −3 through day 0); Peak = peak axitinib exposure (day 12 through day 14); D2 = Day 2 of the washout period (day 16); D7 = Day 7 of the washout period (day 21). Because not all patients are fully evaluable at each time point, the number of patients included in each analysis is given

**Fig. 4** Individual patients' change in plasma VEGF levels during cycle 1. Note that in nearly every case, VEGF levels increased during treatment and decreased during withdrawal

Discussion

We observed a significant increase in tumor proliferation—as assessed by changes in FLT PET uptake—during the withdrawal period of axitinib treatment. This increase may offer an explanation for the negative results of the trials combining VEGFR TKI therapy with cytotoxic chemotherapy conducted thus far, and insights from the present study may lead to the development of a treatment regimen with greater efficacy.

This study was prospectively designed not only to observe potential axitinib withdrawal flare, but to further characterize its temporal dynamics. A previous study of the agent sunitinib [12] was the first to quantify changes in tumor proliferation during TKI therapy and withdrawal, using FLT PET imaging. In the present study, similar imaging time points were chosen, to allow direct comparison between sunitinib and axitinib FLT response (cohort A). Due to the much shorter half-life of axitinib (4–6 h), an additional imaging time point was included at two days of withdrawal, to evaluate the temporal dynamics of the withdrawal flare (cohort B). For all patients, the primary endpoint was to assess proliferative changes over the entire withdrawal period.

Axitinib showed similar effects in terms of both pharmacodynamics and pharmacokinetics to those previously observed for sunitinib [12], with comparable changes in SUV metrics, VEGF levels, and drug PK observed for both agents over the course of a 2/1 dosing schedule. These results confirm that withdrawal flare as assessed with FLT PET imaging is consistent across the two VEGFR inhibitors. The greatest change in tumor FLT uptake was found to occur within 2 days of axitinib withdrawal (SUV_{max} +17 %, *p* = 0.032; SUV_{mean} +14 %, *p* = 0.019), which constitutes approximately ten half-lives of axitinib. By contrast, relatively little change in FLT uptake is observed between day 2 and day 7 of washout (SUV_{max} +6 %, *p* = 0.193; SUV_{mean} +2 %, *p* = 0.232).

Although these results indicate significant proliferative flare over the entire patient population, inspection of individual patients' response (dotted lines in Fig. 3) reveals substantial inter-patient heterogeneity: For some patients, only modest or no withdrawal flare was observed, while other patients experienced substantial withdrawal flare. There is no doubt explained in part by the heterogeneous patient population (Table 1), yet when results are broken out by primary tumor type, no obvious trends emerge linking any one particular tumor type to withdrawal flare (results not shown). In fact, this variety in patients experiencing withdrawal flare serves to demonstrate that it is not a phenomenon unique to any one tumor type, but rather a general response that certain patients have to intermittent dosing of anti-angiogenic therapy, independent of tumor type.

This heterogeneity has implications for the use of treatment holidays. In a prospective study of lung cancer patients, cessation of TKI therapy was associated with a clinically significant risk of accelerated disease progression [1]. The study, which investigated the use of the drug crizotinib, also found the median time to disease flare after TKI discontinuation was 8 days (~4.5 half-lives) [1]. A similar pattern was revealed in the exploratory clinical benefit analysis included in the present study. A higher proportion of patients experiencing clinical benefit showed no significant difference in FLT uptake at the end of washout, relative to peak axitinib concentration. One possible explanation for this difference is that patients whose tumors show a greater ability to adapt to anti-angiogenic therapy (e.g., by mounting a proliferative flare response) may face a worse prognosis, due to the activation of escape pathways. This could account for the association between withdrawal flare and poor clinical outcome. However, due to the small number of evaluable patients who responded favorably to axitinib treatment ($n = 4$), this study is not sufficiently powered to test this hypothesis.

As noted by Chaft et al. [1], the incidence of disease flare is currently unknown, and it is impossible to predict who will experience it. It has therefore been recommended that drug holidays should be eliminated, to avoid the risk of disease flare and thus the increased risk of rapid progression and poor survival. In the recent CAIRO3 study, maintenance therapy with capecitabine and the VEGF inhibitor bevacizumab was found to confer an improvement in progression-free survival [10], prompting consideration of whether treatment with anti-VEGF agents should be continued, in hopes of dampening any significant tumor proliferation, thus avoiding the rapid progression that can occur with treatment cessation. However, the results of this FLT PET analysis may support a different approach. The increased FLT uptake during withdrawal suggests that a higher proportion of

tumor cells may have entered the S-phase in response to axitinib cessation. Thus, a sequential intervention using an S-phase-specific chemotherapy agent may be effective as early as 2 days post-cessation of axitinib therapy, as the tumor will have already experienced the majority of its increase in proliferation.

Plasma VEGF levels also help to characterize and further highlight potential mechanisms of the disease flare. In another previous study of the agent sunitinib, plasma VEGF levels were found to increase by threefold during the first cycle of treatment and then return to baseline levels during the scheduled treatment break [4]. However, the plasma VEGF level rose progressively higher during each subsequent cycle of sunitinib therapy. This ratcheting up of VEGF response may be a driver of tumor resistance to sunitinib, as an increasingly strong angiogenic signal is produced in response to sunitinib cessation. In our study, patients were treated with axitinib on an intermittent (2-week-on/1-week-off) schedule only during the first cycle; axitinib was given continuously beginning with cycle 2. Although VEGF levels were found to increase during axitinib therapy and decline during washout, we did not observe a comparable ratcheting effect. Plasma VEGF levels were no higher during cycle 3 than they were at peak drug exposure during cycle 1 ($p = 0.42$). This suggests a stable VEGF level through three cycles of treatment, leading to the hypothesis that axitinib may be a more sustainable option for managing the compensatory resistance mechanisms represented by the rise in VEGF observed in response to sunitinib treatment.

Based in part on the results presented here, two new trials have been initiated at the University of Wisconsin. We have an ongoing trial to repeat the imaging sequence during the third cycle of axitinib therapy, administering axitinib on a 2/1 schedule for 3-week cycles. The relative stability of plasma VEGF levels observed in this study can then be compared with the new study, in which each cycle will contain intermittent dosing. We are conducting another clinical trial evaluating the sequential combination of the novel TKI (X-82) with a short half-life (<8 h) with a cytotoxic chemotherapy agent (docetaxel) in order to capitalize on the tumor flare phenomenon. By coupling a cytotoxic agent during the washout period, we plan to determine whether efficacy can be improved by delivering a sequential combination of these two drugs.

Acknowledgments Peter Scully was supported by NIH Grant Number 5T32CA009206 (T32 training grant). This clinical trial was funded by a Pfizer Investigator-Initiated Research Award (133-PRJ17VG).

Conflict of interest The authors have no conflicts of interest to disclose.

Ethical standard All procedures performed in studies involving human participants were in accordance with the ethical standards of the institutional and/or national research committee and with the 1964 Helsinki Declaration and its later amendments or comparable ethical standards.

References

1. Chaft JE, Oxnard GR, Sima CS, Kris MG, Miller VA, Riely GJ (2011) Disease flare after tyrosine kinase inhibitor discontinuation in patients with EGFR-mutant lung cancer and acquired resistance to erlotinib or gefitinib: implications for clinical trial design. *Clin Cancer Res* 17:6298–6303
2. Chalkidou A, Landau DB, Odell EW, Cornelius VR, O'Doherty MJ, Marsden PK (2012) Correlation between Ki-67 immunohistochemistry and 18F-fluorothymidine uptake in patients with cancer: a systematic review and meta-analysis. *Eur J Cancer* 48:3499–3513
3. Cobleigh MA, Langmuir VK, Sledge GW, Miller KD, Haney L, Novotny WF, Reimann JD, Vassel A (2003) A phase I/II dose-escalation trial of bevacizumab in previously treated metastatic breast cancer. *Semin Oncol* 30:117–124
4. Deprimo SE, Bello CL, Smeraglia J, Baum CM, Spinella D, Rini BI, Michaelson MD, Motzer RJ (2007) Circulating protein biomarkers of pharmacodynamic activity of sunitinib in patients with metastatic renal cell carcinoma: modulation of VEGF and VEGF-related proteins. *J Transl Med* 5:32
5. Escudier B, Eisen T, Stadler WM, Szczylik C, Oudard S, Siebels M, Negrier S, Chevreau C, Solska E, Desai AA, Rolland F, Demkow T, Hutson TE, Gore M, Freeman S, Schwartz B, Shan M, Simantov R, Bukowski RM, Group TS (2007) Sorafenib in advanced clear-cell renal-cell carcinoma. *N Engl J Med* 356:125–134
6. Folkman J (2003) Angiogenesis inhibitors: a new class of drugs. *Cancer Biol Ther* 2:S127–S133
7. Folkman J (2003) Fundamental concepts of the angiogenic process. *Curr Mol Med* 3:643–651
8. Gordon MS, Margolin K, Talpaz M, Sledge GW Jr, Holmgren E, Benjamin R, Stalter S, Shak S, Adelman D (2001) Phase I safety and pharmacokinetic study of recombinant human anti-vascular endothelial growth factor in patients with advanced cancer. *J Clin Oncol* 19:843–850
9. Kindler HL, Ioka T, Richel DJ, Bennouna J, Letourneau R, Okusaka T, Funakoshi A, Furuse J, Park YS, Ohkawa S, Springett GM, Wasan HS, Trask PC, Bycott P, Ricart AD, Kim S, Van Cutsem E (2011) Axitinib plus gemcitabine versus placebo plus gemcitabine in patients with advanced pancreatic adenocarcinoma: a double-blind randomised phase 3 study. *Lancet Oncol* 12:256–262
10. Koopman M, Simkens L, May A, Mol L, van Tinteren H, Punt C (2014) Final results and subgroup analyses of the phase 3 CAIRO3 study: Maintenance treatment with capecitabine and bevacizumab versus observation after induction treatment with chemotherapy and bevacizumab in metastatic colorectal cancer (mCRC). *J Clin Oncol* 32, (suppl 3; abstr LBA388)
11. Kuriyama Y, Kim YH, Nagai H, Ozasa H, Sakamori Y, Mishima M (2013) Disease flare after discontinuation of crizotinib in anaplastic lymphoma kinase-positive lung cancer. *Case Rep Oncol* 6:430–433
12. Liu G, Jeraj R, Vanderhoek M, Perlman S, Kolesar J, Harrison M, Simoncic U, Eickhoff J, Carmichael L, Chao B, Marnocha R, Ivy P, Wilding G (2011) Pharmacodynamic study using FLT PET/CT in patients with renal cell cancer and other solid malignancies treated with sunitinib malate. *Clin Cancer Res* 17:7634–7644
13. Lovet JM, Ricci S, Mazzaferro V, Hilgard P, Gane E, Blanc JF, de Oliveira AC, Santoro A, Raoul JL, Forner A, Schwartz M, Porta C, Zeuzem S, Bolondi L, Greten TF, Galle PR, Seitz JF, Borbath I, Haussinger D, Giannaris T, Shan M, Moscovici M, Voliotis D, Bruix J, Group SIS (2008) Sorafenib in advanced hepatocellular carcinoma. *N Engl J Med* 359:378–390
14. Motzer RJ, Hutson TE, Tomczak P, Michaelson MD, Bukowski RM, Oudard S, Negrier S, Szczylik C, Pili R, Bjamason GA, Garcia-del-Muro X, Sosman JA, Solska E, Wilding G, Thompson JA, Kim ST, Chen I, Huang X, Figlin RA (2009) Overall survival and updated results for sunitinib compared with interferon alfa in patients with metastatic renal cell carcinoma. *J Clin Oncol* 27:3584–3590
15. Rini BI (2005) SU11248 and AG013736: current data and future trials in renal cell carcinoma. *Clin Genitourin Cancer* 4:175–180
16. Rini BI, Escudier B, Tomczak P, Kaprin A, Szczylik C, Hutson TE, Michaelson MD, Gorbunova VA, Gore ME, Rusakov IG, Negrier S, Ou YC, Castellano D, Lim HY, Uemura H, Tarazi J, Cella D, Chen C, Rosbrook B, Kim S, Motzer RJ (2011) Comparative effectiveness of axitinib versus sorafenib in advanced renal cell carcinoma (AXIS): a randomised phase 3 trial. *Lancet* 378:1931–1939
17. Rini BI, Wilding G, Hudes G, Stadler WM, Kim S, Tarazi J, Rosbrook B, Trask PC, Wood L, Dutcher JP (2009) Phase II study of axitinib in sorafenib-refractory metastatic renal cell carcinoma. *J Clin Oncol* 27:4462–4468
18. Rugo HS, Herbst RS, Liu G, Park JW, Kies MS, Steinfeldt HM, Pithavala YK, Reich SD, Freddo JL, Wilding G (2005) Phase I trial of the oral antiangiogenesis agent AG-013736 in patients with advanced solid tumors: pharmacokinetic and clinical results. *J Clin Oncol* 23:5474–5483
19. Rugo HS, Stopeck AT, Joy AA, Chan S, Verma S, Lluch A, Liau KF, Kim S, Bycott P, Rosbrook B, Bair AH, Soulieres D (2011) Randomized, placebo-controlled, double-blind, phase II study of axitinib plus docetaxel versus docetaxel plus placebo in patients with metastatic breast cancer. *J Clin Oncol* 29:2459–2465
20. Senger DR, Galli SJ, Dvorak AM, Perruzzi CA, Harvey VS, Dvorak HF (1983) Tumor cells secrete a vascular permeability factor that promotes accumulation of ascites fluid. *Science* 219:983–985
21. Sonpavde G, Hutson TE, Rini BI (2008) Axitinib for renal cell carcinoma. *Expert Opin Investig Drugs* 17:741–748
22. Sternberg CN, Szczylik C, Lee E, Salman PV, Mardiak J, Davis ID, Pandite L, Chen M, McCann L, Hawkins R (2009) A randomized, double-blind phase III study of pazopanib in treatment-naïve and cytokine-pretreated patients with advanced renal cell carcinoma (RCC). *J Clin Oncol* 27
23. Therasse P, Arbuck SG, Eisenhauer EA, Wanders J, Kaplan RS, Rubinstein L, Verweij J, Van Glabbeke M, van Oosterom AT, Christian MC, Gwyther SG (2000) New guidelines to evaluate the response to treatment in solid tumors. European organization for research and treatment of cancer, national cancer institute of the United States, national cancer institute of Canada. *J Natl Cancer Inst* 92:205–216
24. van der Graaf WT, Blay JY, Chawla SP, Kim DW, Bui-Nguyen B, Casali PG, Schoffski P, Aglietta M, Staddon AP, Beppu Y, Le Cesne A, Gelderblom H, Judson IR, Araki N, Ouali M, Marreand S, Hodge R, Dewji MR, Coens C, Demetri GD, Fletcher CD, Dei Tos AP, Hohenberger P, Tissue ES, Bone Sarcoma G, group Ps, (2012) Pazopanib for metastatic soft-tissue sarcoma (PAL-ETTE): a randomised, double-blind, placebo-controlled phase 3 trial. *Lancet* 379:1879–1886
25. Wahl RL, Jacene H, Kasamon Y, Lodge MA (2009) From RECIST to PERCIST: evolving Considerations for PET response criteria in solid tumors. *J Nucl Med* 50(Suppl 1):122S–150S
26. Yun KJ, Kim W, Kim EH, Kim MH, Lim DJ, Kang MI, Cha BY (2014) Accelerated disease progression after discontinuation of sorafenib in a patient with metastatic papillary thyroid cancer. *Endocrinol Metab (Seoul)* 29:388–393